IEEE Access
Multidisciplinary | Rapid Review | Open Access Journal

Received December 3, 2019, accepted January 5, 2020, date of publication January 9, 2020, date of current version January 17, 2020.

Digital Object Identifier 10.1109/ACCESS.2020.2965174

Fuzzy-Based Histogram Partitioning for Bi-Histogram Equalisation of Low Contrast Images

MOHAMMAD FARHAN KHAN[1], DEEPALI GOYAL[2], MUAFFAQ M. NOFAL[3], EKRAM KHAN[2], RAMI AL-HMOUZ[4], AND ENRIQUE HERRERA-VIEDMA[4,5]

[1]Department of Electrical Engineering, IIT Roorkee, Roorkee 247667, India
[2]Department of Electronics Engineering, Aligarh Muslim University, Aligarh 202002, India
[3]Department of Mathematics and General Sciences, Prince Sultan University, Riyadh 11586, Saudi Arabia
[4]Department of Electrical and Computer Engineering, King Abdulaziz University, Jeddah 21589, Saudi Arabia
[5]Andalusian Research Institute in Data Science and Computational Intelligence, University of Granada, 18071 Granada, Spain

Corresponding author: Mohammad Farhan Khan (farhan7787@gmail.com)

This work was supported by the Deanship of Scientific Research (DSR), King Abdulaziz University, Jeddah, under Grant DF-374-135-1441.

ABSTRACT The conventional histogram equalisation (CHE), though being simple and widely used technique for contrast enhancement, but fails to preserve the mean brightness and natural appearance of images. Most of the improved histogram equalisation (HE) methods give better performance in terms of one or two metrics and sacrifice their performance in terms of other metrics. In this paper, a novel fuzzy based bi-HE method is proposed which equalises low contrast images optimally in terms of all considered metrics. The novelty of the proposed method lies in selection of fuzzy threshold value using level-snip technique which is then used to partition the histogram into segments. The segmented sub-histograms, like other bi-HE methods, are equalised independently and are combined together. Simulation results show that for wide-range of test images, the proposed method improves the contrast while preserving other characteristics and provides good trade-off among all the considered performance metrics.

INDEX TERMS Contrast enhancement, histogram equalisation, image transformation, fuzzy membership function, dynamic range, optimal threshold.

I. INTRODUCTION

The availability of external light source is one of the important factor that affects the appearance of images. It has been observed that images may completely be washed-out due to over-exposure of external light (image with large number of bright pixels) or may appear very dark due to insufficient light intensity (image with large number of dark pixels). In each case, the resulting images are of poor contrast and many image details are hardly visible. The sensitivity of camera sensors also affects the quality of images. The inferior sensitivity of charge coupled device/complementary metal oxide semiconductor (CCD/CMOS) sensors usually fail to capture entire available dynamic range, resulting in poor contrast and the details of the images appear less appealing [1], [2]. Consequently, the contrast enhancement techniques are used to improve the quality of such low-contrast images.

The contrast enhancement has also found its application in biomedical imaging for computer aided diagnosis of various disease such as detection of malignant/benign lesions, knee joint ailment etc. The classification/detection of diagnostically small lesions is a challenging task in machine learning due to the small variation in intensities across the lesion's edge with respect to its surrounding. The contrast enhancement of such images before applying machine learning algorithm are useful in detecting the small lesions [3]–[5]. Furthermore, the significant role of contrast enhancement has also been observed in tracking the objects under low visibility conditions when the object are not clearly visible or differentiable in images or videos [6].

The conventional histogram equalisation (CHE) technique is one of the widely used, simple and effective method for

The associate editor coordinating the review of this manuscript and approving it for publication was Haimiao Hu.

image contrast enhancement [7]. In CHE, the input intensity levels are transformed to other intensity levels by using the cumulative distribution function (cdf) of input image as a mapping function. It achieves overall contrast enhancement by stretching its occupied intensity range to the full dynamic range, that is, $[0, 2^n-1]$ for n-bit/pixel image. Although CHE has been considered as an efficacious method, it either shifts the mean brightness of the image or over enhances some regions of the image, resulting in loss of natural appearances of image. To overcome these limitations and to control the level of contrast enhancement in processed images, various improved HE methods have been suggested in the literature [8]–[36]. These methods can be broadly classified into two major categories namely bi-H and multi-HE methods depending on the number of segments the image histogram is partitioned. The HE methods in each category can further be classified into two sub-categories depending on the modifications in sub-histograms before applying the equalisation process. The first sub-category includes simple threshold based histogram partitioning followed histogram equalisation (HE) of each sub-histogram without any pre-processing [8]–[13], [17], [18], [27], [28], whereas in the second category the HE methods use pre-histogram controllers that modify the characteristics of sub-histograms before the equalisation process [14]–[16], [19]–[24].

A number of bi-HE methods have been designed to preserve the brightness of the input image by segmenting image histogram into small sub-histograms using mean (or median) intensity as threshold value, and equalising each sub-histogram independently [8]–[11]. These methods mainly suffer from the intensity saturation problem and excessive shifting of high peak regions of the histogram during enhancement process, resulting in the loss of information (entropy value) and natural appearance due to excessive shifting of mean brightness value of the histogram in the processed images. To overcome these limitations, many advance HE methods are being developed that enhances the contrast of the input image either by maximising the entropy of the output image [12], [13], or by pre-process the input histogram (or use pre-histogram controller) before equalisation to avoid the excessive shifting of high peak regions in the output histogram [14]–[16].

To overcome the drawbacks of bi-HE methods, a number of multi-HE methods have been suggested [17]–[24]. Among them the recursive mean-separate histogram equalisation (RMSHE) [17] and recursive sub-image histogram equalisation (RSIHE) [18] are the most popular as they are direct extensions of corresponding bi-HE methods namely BBHE [10] and DSIHE [11] methods respectively. These multi-HE methods control the brightness shift in the processed images to preserve the brightness and natural appearance, but at the cost of increased complexity and reduced contrast enhancement compared to CHE and bi-HE methods. Furthermore, it has been observed that the applying equalisation process to the large number of segments may not expand the dynamic range effectively resulting into severe saturation problem which in turn lead to the visual artifacts in the processed images. Recently dynamic HE methods has been introduced to overcome the intensity saturation problem in the processed images by stretching the image histogram before the equalisation [19]–[24]. The relatively inferior contrast enhancement property of mlti-HE methods in comparison to CHE and b-HE methods is undesirable for many applications where processed histogram with larger variance is required.

The fuzzy-based rules are also applied in histogram equalisation process to control excessive brightness shift in the processed images. The fuzzy HE (FHE) methods usually transform crisp histogram to a fuzzy histogram and use statistical approaches for histogram segmentation [23], [25], [26]. It has been observed that fuzzy histogram may handle the imprecision in intensity levels and can deliver smooth histogram for hassle-free partitioning [23]. The role of fuzzy histogram in equalisation process has been studied to some extent [29], [32]–[39], but to the best of our knowledge, it's application for finding optimal threshold for histogram partitioning in bi- or multi-HE methods has not yet been explored. Therefore this paper proposes the use of fuzzy logic in searching the optimal threshold for histogram partitioning for bi-HE methods.

A. MOTIVATION

It has been observed that BBHE [10] and DSIHE [11] techniques which segments the image histogram into two non-overlapping segments by considering the mean and median of the input image as threshold respectively and then applying the CHE on each histogram segment independently, may not always result into the best performance of bi-HE methods for all metrics. In order to justify the validity of our claims, two images are selected from the database of 100 training images used in this work. Fig. 1 illustrates the impact of varying the threshold intensity levels on the performance of bi-HE method, measured in terms of six metrics namely mean brightness, entropy (E), standard deviation (SD), edge based contrast measurement (EBCM) [40], universal image quality (UIQ) [41] and peak signal to noise ratio (PSNR). Note that, all the metrics for each image have been normalised on the scale of [0,1] and plotted in same graph for better data visualisation.

It can be observed from Figs. 1(a)-(b) that for both images, BBHE and DSIHE methods does not always gives the best performance for all considered metrics by selecting the mean and median values as threshold for histogram segmentation. Further, a close observation of Table 1 reveals that the threshold for best performance value of all metrics lie closer to either mean of the input image rather than exactly on mean values. For example, for ID0001 image, best performance in terms of SD and E are obtained when threshold value is below but close to input mean value; while for other metrics namely mean absolute difference (or absolute mean error), PSNR, UIQ and EBCM, the best performance is obtained at the threshold values that are higher than input mean value.

TABLE 1. Deviation of threshold value from its mean(μ) leading to best performance value for different metrics for two test images ID0001 and ID0004.

Test images	Best performance threshold values					
	AMBE	E (bits)	SD	EBCM	UIQ	PSNR (dB)
Car or ID0001 ($\mu < L/2$)	μ+1	μ−8	μ−1	μ+3	μ+4	μ+20
Rock or ID0004 ($\mu \geq L/2$)	μ−18	μ+15	μ+14	μ+14	μ−15	μ−15

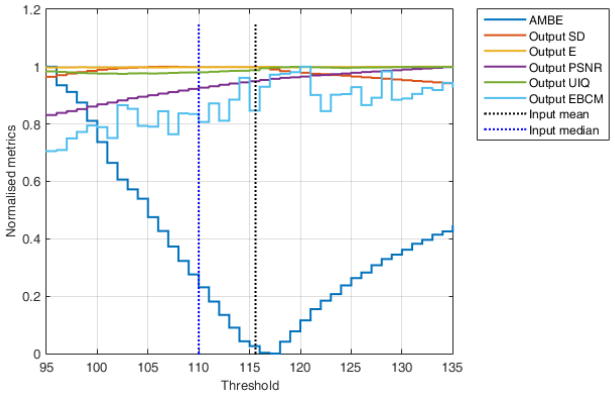

(a) ID0001

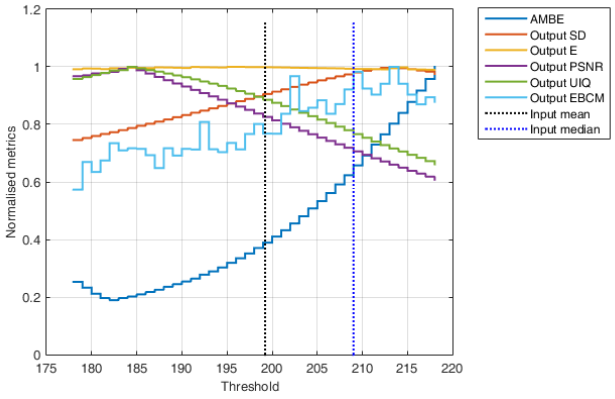

(b) ID0004

FIGURE 1. Impact of varying threshold intensity for histogram segmentation on the performance of bi-HE method that has been estimated using six performance evaluation metrics (AMBE, SD, E, PSNR, UIQ and EBCM) for images: (a) ID0001 and (b) ID0004.

An almost inverse observation can be inferred for ID0004 image.

Furthermore, for data set of 100 gray-scale images, we have observed that for images having mean intensity value (μ) below $L/2$ (where L is total number of discrete levels of the image), the best performance of bi-HE method in terms of absolute mean brightness error (AMBE), EBCM, UIQ and PSNR are obtained at threshold value greater than the image mean, whereas the best performance in terms of E and SD are obtained for threshold value slightly lower than the image mean. The case is reversed for the images with $\mu \geq L/2$.

From these observations, it can be asserted that mean/median based bi-HE methods (namely BBHE/DSIHE) do not necessarily have their best performance, rather the optimal threshold value (threshold at which the best performance is obtained) varies from criterion to criterion. Though optimal threshold lies around the mean/median but not exactly on mean/median. Therefore it is obvious that a mean or median-based thresholding does not give optimal performance of bi-HE methods for all metrics. Therefore, there is a need to develop a new methodology to obtain a threshold value that gives optimal performance for all metrics.

Hence, in this work, we have used a fuzzy-based approach that uses a customised membership function depending on image's mean intensity value and introduced a novel snipping process for that membership function. The snipping process clips the membership function, and if the function is negatively skewed for $\mu < L/2$ then the threshold value will be more but closer to the image mean intensity. While the case is reverse for $\mu \geq L/2$, as a positively skewed membership function will be selected to obtain threshold value near to but less than the image mean intensity value.

B. CONTRIBUTION

In this paper, a novel fuzzy-based threshold selection criterion is suggested for histogram partitioning to perform bi-HE on low-contrast images, which aimed to focus on enhancing the low contrast images by finding an optimal threshold that can equally favour all performance metrics instead of focusing on accomplishment of one or two metric(s) out of all. Unlike other HE methods, the main feature of the proposed bi-HE method lies in its optimal performance in terms of all considered parameters. This optimal performance is in contrast to that of existing bi-HE methods namely BBHE and DSIHE [10], [11], which are not able to satisfy all requirements such as contrast improvement, natural preservation and maintain the mean intensity value in processed images. The proposed technique is also extended to colour images, in which colour images are first transformed to HSV colour model and proposed algorithm is applied to the luminance (V) component only.

C. ORGANISATION OF PAPER

The rest of the paper is organised as follows. Section II contains the details of the proposed algorithm. Section III includes results for wide range of images taken from various data sets and relevant discussions. In Section IV, the proposed method is extended to colour images and its performance for colour image enhancement is reported. Finally, the paper is concluded in Section V.

II. PROPOSED FUZZY-BASED BI-HE METHOD

As stated earlier, the focus of present work is to develop a novel fuzzy-based algorithm to find a threshold for histogram partitioning, which can provide an optimal trade-off among various performance metrics, as mean/median based threshold is not always a better choice. The main objective of proposed method is to obtain an appropriate threshold value to segment image histogram into sub-histograms for bi-HE methods, so that desirable objective and subjective quality can be achieved. For this purpose the proposed method utilises fuzzy logic with asymmetrical triangular membership function. The details of steps involved in the proposed method are discussed in the following sub-sections.

A. FUZZY-BASED THRESHOLD SELECTION

The novelty of the proposed method lies in finding fuzzy-based threshold for histogram partitioning in bi-HE methods. The proposed method uses two customised (one positively and one negatively skewed) triangular membership functions (MFs), the parameters of which are determined from the mean and standard deviation of image intensity. The range of possible values of threshold (middle value of this range is considered as threshold) is obtained by overlapping ranges obtained from each of two the MFs using fuzzy level-snip approach.

1) MEMBERSHIP FUNCTIONS (MFS) AND FUZZY RULES

The first step in the proposed method is to design suitable membership functions. Though the symmetrical triangular membership functions are widely used in fuzzy theory, in this work we propose to use two asymmetrical triangular functions, each skewed for one of sloped lines, called negatively and positively skewed triangular fuzzy membership function respectively. Two statistical parameters namely mean brightness (μ) and standard deviation (σ) of input image (I) are used to compute the edges of these MFs. Our observations over a large image data set reveal that the threshold for histogram partitioning offering the best performance of six considered metrics mostly lie within the range of $[\mu - \sigma, \mu + \sigma]$. The μ and σ of a given input I can be evaluated according to Eqns. (1) and (2) respectively.

$$\mu = \sum_{x_k=x_l}^{x_h} x_k \times \frac{n(x_k)}{N} \tag{1}$$

$$\sigma = \sqrt{\sum_{x_k=0}^{L-1} (x_k - \mu)^2 \times \frac{n(x_k)}{N}} \tag{2}$$

where $n(x_k)$ is total number of pixels with k^{th} intensity, N is total number of pixels in the image, and x_l and x_h are the lowest and highest intensity levels of the image respectively. The asymmetrical (skewed) triangular MFs can be described in terms of three variables, namely a_1, a_2, and a_3, called fuzzy numbers, which determines the spatial coordinates of three vertices of MF, as expressed in Eqn. (3).

$$f(x) = \begin{cases} 0, & x \le a_1 \\ \dfrac{x - a_1}{a_2 - a_1}, & a_1 \le x \le a_2 \\ \dfrac{a_3 - x}{a_3 - a_2}, & a_2 \le x \le a_3 \\ 0, & x \ge a_3 \end{cases} \tag{3}$$

The values of a_1 and a_3 are fixed as $\mu-\sigma$ and $\mu+\sigma$ respectively, whereas the value of a_2 depends on the mean value of the input image and skewness of the membership function. The value of a_2 is determined according to following rules (assume $L-1 = 2^n - 1$, where $n = 0$ for black colour and $n = 8$ for white colour in 8-bit gray scale image):

Rule I

a: If $\mu < L/2$, then parameter $a_2 = a_2^- = \mu+\sigma/2$ (negative skewness), for optimising AMBE, EBCM, UIQ and PSNR metrics.

b: If $\mu \ge L/2$, then parameter $a_2 = a_2^+ = \mu-\sigma/2$ (positive skewness), for optimising AMBE, EBCM, UIQ and PSNR metrics.

Rule II

a: If $\mu \ge L/2$, then parameter $a_2 = a_2^- = \mu + \sigma/2$ (negative skewness), for optimising E and SD metrics.

b: If $\mu < L/2$, then parameter $a_2 = a_2^+ = \mu - \sigma/2$ (positive skewness), for optimising E and SD metrics.

Therefore a triangular skewed membership function can be specified by specifying $(a_1, 0)$, $(a_2, 1)$ and $(a_3, 0)$ as three corners of a triangle. After determining the skewed triangular membership function $f(x)$ for each set of the performance metrics, the next step is to determine the range of x (intensity range) in which the optimal threshold for histogram segmentation may lie.

2) FUZZY LEVEL-SNIP

In the proposed work, we use the fuzzy level-snip technique, in which the triangular membership function $f(x)$ is snipped horizontally at a finite level $l \in [0, 1]$. The appropriate value of l is determined using the algorithm whose pseudo code is shown in Algorithm 1 for $\zeta = 100$ training images. The difference between upper and lower values of x for which $f(x) \ge l$ is selected as desirable range of x in which the optimal threshold is to be searched. Let these upper and lower values of x satisfying $f(x) \ge l$ are denoted as $(\lambda_L^l, \lambda_U^l)$, which are shown in Figs. 2(a) and (b) for positively and negatively skewed MFs respectively. For a skewed triangular membership function $f(x)$ with $(a_1, 0)$, $(a_2, 1)$ and $(a_3, 0)$ as coordinates of its three corners, λ_L^l (the value of x at which $f(x) = l$ intersects the line joining corners $(a_1, 0)$ and $(a_2, 1)$) can be determined using eq. 4.

$$\lambda_L^l = a_1 + (a_2 - a_1) \times l \tag{4}$$

Similarly λ_U^l (the value of x at which $f(x) = l$ intersects the line joining corners $(a_2, 1)$ and $(a_3, 0)$, can be determined

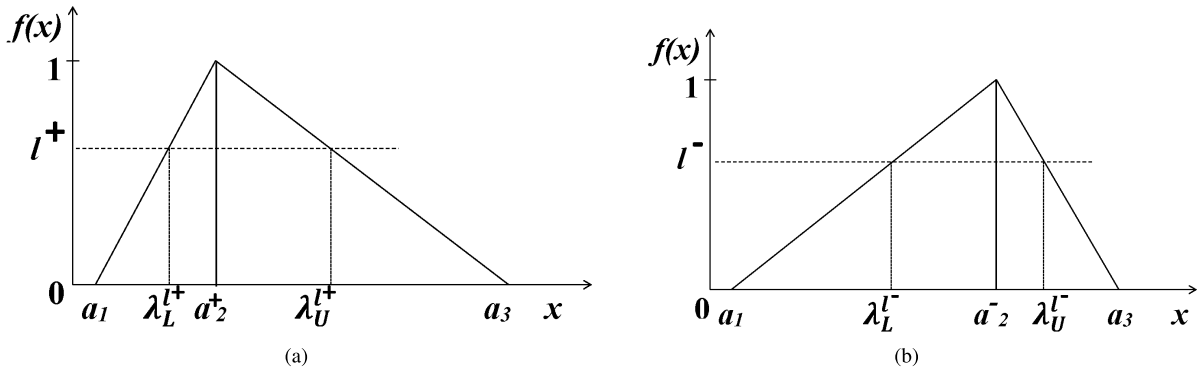

FIGURE 2. A positively and negatively skewed triangular fuzzy MF with level-snip (a) Positively skewed (b) Negatively skewed.

using eq. 5.

$$\lambda_U^l = a_3 - (a_3 - a_2) \times l \tag{5}$$

Since the objective of proposed technique to find suitable threshold for histogram partitioning to achieve optimal performance for multiple criteria, and the triangular membership function to be selected is based on these criteria according to the rules specified above, therefore, it is required to determine λ_L^l and λ_U^l for both positively and negatively skewed triangular MFs, denoted as $(\lambda_L^{l+}, \lambda_U^{l+})$ and $(\lambda_L^{l-}, \lambda_U^{l-})$ respectively as illustrated in Figs. 2(a) and (b).

3) THRESHOLD SELECTION

After determining the lower and upper ranges of intensities from the level-snips of positively and negatively skewed triangular MFs i.e. $(\lambda_L^{l+}, \lambda_U^{l+})$ and $(\lambda_L^{l-}, \lambda_U^{l-})$, the next step is to determine the intensity range that is common in two MFs and then the statistical mean of this common range is selected as desired fuzzy threshold t. Let λ_L and λ_U are the lower and upper limits of the common range, where $\lambda_L = max(\lambda_L^{l-}, \lambda_L^{l+})$ and $\lambda_U = min(\lambda_U^{l-}, \lambda_U^{l+})$. The fuzzy threshold t is then determined as follows:

$$t = \sum_{x_k=\lambda_L}^{\lambda_U} x_k \times p(x_k) \tag{6}$$

where, $p(x_k)$ is the probability distribution function (pdf) of k^{th} intensity level x_k. It should be noted that, the purpose of opting two skewed asymmetrical triangular membership functions is to adjust λ_L and λ_U, and therefore the threshold t according to snip level l, which is otherwise not possible in a symmetrical triangular membership functions. Note that, the novelty of the work lies in the selection of optimum value of the threshold t (which is a mean value of intersecting region between two differently skewed MF's) that solely depends on snip levels l^+ and l^- which help in estimating λ_L^{l+}, λ_U^{l+}, λ_L^{l-} and λ_U^{l-}; and eventually the values of different λ's are used to find the common or intersecting region between both differently skewed MF's.

B. HISTOGRAM SEGMENTATION AND EQUALISATION

In a bi-HE method, once the optimal threshold intensity 't' (as defined in Eqn. (6)) is determined, the histogram $H(x_k)$ $(= n(x_k)$, where $k \in [0, L-1])$ of the input image I can be segmented into two sub-histograms, namely lower and upper sub-histograms i.e. $H_L(x_k)$ and $H_U(x_k)$ respectively (refer to Eqns. (7) and (8)), where $x_k \in [0, L-1]$, L is the maximum intensity level.

$$H_L(x_k) = \begin{cases} H(x_k), & \text{if } x_k \in [0, t] \\ 0, & otherwise \end{cases} \tag{7}$$

and

$$H_U(x_k) = \begin{cases} H(x_k), & \text{if } x_k \in [t+1, L-1] \\ 0, & otherwise \end{cases} \tag{8}$$

It should be noted that $H_L(x_k) \cup H_U(x_k) = H(x_k)$ and $H_L(x_k) \cap H_U(x_k) = \emptyset$. Two sub-images, one corresponding to each segmented sub-histogram, are then equalised independently using conventional HE method. The T_L and T_U, the transformation functions used to equalise lower and upper sub-histograms (or sub-images) respectively, are defined in Eqns. (9) and (10) as:

$$T_L(x_k) = |t \times \sum_{x_k=0}^{t} p_L(x_k)| \tag{9}$$

$$T_U(x_k) = (t+1) + |\{(L-1) - (t+1)\} \times \sum_{x_k=t+1}^{L-1} p_U(x_k)| \tag{10}$$

where, $|\cdot|$ rounds rational number to nearest gray scale value, and $p_L(x_k)$ and $p_U(x_k)$ are probability distribution function of $H_L(x_k)$ and $H_U(x_k)$ respectively.

C. ESTIMATION OF SNIPPING LEVELS

As mentioned earlier, the performance of the proposed algorithm solely depends on estimation of optimal values of snipping levels l^+ and l^-. The value of both levels has been estimated by training the algorithm over the data set of 100 images. The metrics that have been used to train the

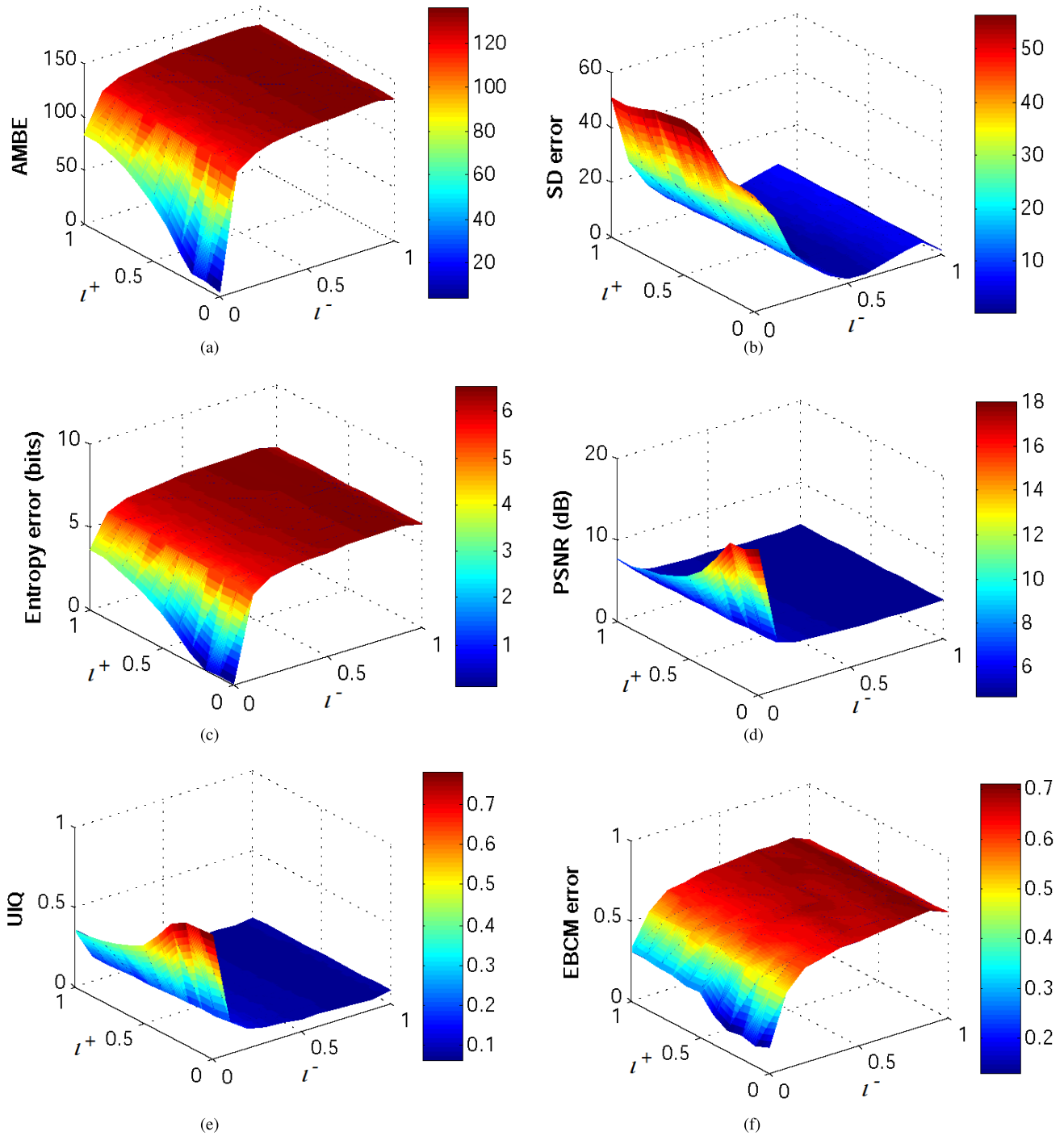

FIGURE 3. Variation in performance of different metrics for image ID0001 for different fuzzy level-snips.

algorithm are AMBE, SD error, E error, PSNR, UIQ and EBCM error. In order to estimate the optimal value of levels l^+ and l^-, firstly for each training image, all possible values of l ranging from 0 to 1 with step size of 10^{-1} are considered and the values of all six metrics are recorded against each combination of l^+ and l^-. Since the value of threshold t, calculated using 6 for each training image changes according to the selected combination of the snipping levels l^+ and l^-, for each image the combination of l^+ and l^- values that gives the best value of corresponding performance metrics are noted, and finally the averaged value (of 100 training images) is considered for further evaluation. The pseudo-code of the optimisation routine for estimating final value of l^+ and l^- is given in Algorithm-1. Fig. 3 illustrates the

Algorithm 1 Pseudo Code of Optimisation Algorithm Using a Training Database Having ζ Number of Images

Data: $I(\upsilon)$, where $\upsilon = 1 : \zeta$
Result: Final optimum values of l^- and l^+
Initialise;
Load data set $I(\upsilon)$;
for $\upsilon = 1 : \zeta$ **do**
  Calculate $\mu(\upsilon)$ and $\sigma(\upsilon)$;
  Calculate triangular fuzzy nos. $z(\upsilon) = (a_1, a_2, a_3)$;
  Set $a_1 = \mu(\upsilon) - \sigma(\upsilon)$ and $a_3 = \mu(\upsilon) + \sigma(\upsilon)$;
  for $l^- = 0 : 1$ with step-size= 10^{-1} **do**
    Set $a_2 = \mu(\upsilon) + \sigma(\upsilon)/2$;
    Calculate λ_L^{l-} and λ_U^{l-};
    for $l^+ = 0 : 1$ with step-size= 10^{-1} **do**
      Set $a_2 = \mu(\upsilon) - \sigma(\upsilon)/2$;
      Calculate λ_L^{l+} and λ_U^{l+};
      Evaluate $t(v) = \sum_{x_k(v)=\lambda_L}^{\lambda_U} x_k(v) \times p(x_k(v))$;
      Segment histogram $H(I(\upsilon))$ via $t(\upsilon)$;
      Apply transformation process (T) over sub-histograms;
      Get output image $O(\upsilon) = T(I(\upsilon))$;
      Record AMBE, SD error, E error, PSNR, UIQ and EBCM error;
    end
  end
  Extract and save best combination of l^- and l^+ giving optimal performance for six metrics;
end
Get final average values of l^- and l^+.

outcome of optimisation routine for ID0001 image. From Fig. 3(a)-(f), the best combination value of levels l^+ and l^- lies in the region near zero. The proposed optimisation routine is applied to all 100 test images to estimate the best performance values of l^+ and l^- for each image, and then finally averaged to find the optimal values of l^+ and l^-.

III. RESULTS AND DISCUSSIONS

The proposed algorithm and its optimisation routine (Algorithm-1) are implemented in MATLAB R2013b and executed on a PC equipped with Core i7 3.06GHz processor and 32 GB of RAM. The optimal average values of l^- and l^+ estimated over a training set of 100 images are come out to be 0.1385 and 0.2515 respectively; which are then used for testing purpose on data set of 1000 images.

A. DATA SET

The core objective of the proposed algorithm is to enhance the contrast of diverse natural images, that have wide variation in statistical specifications along with variation in appearances. The data set considered in this study includes dissimilar set of images which can be broadly classified into ariel, texture, sequence, plant, under water, remotely sensed images etc. One of the reasons behind opting such wide class of data set is to quantify diversity of the natural images. The four metrics that define the training set are mean, SD, E (bits) and EBCM having average value of 131.27, 35.81, 6.62 and 0.20 respectively. On the other hand, the average mean, SD, E (bits) and EBCM value of test image data set is 136.26, 45.56, 6.55 and 0.13 respectively. It is worth noting that, the difference in the average values between metrics of both data sets (training and test) represents diversity of randomly selected data sets.

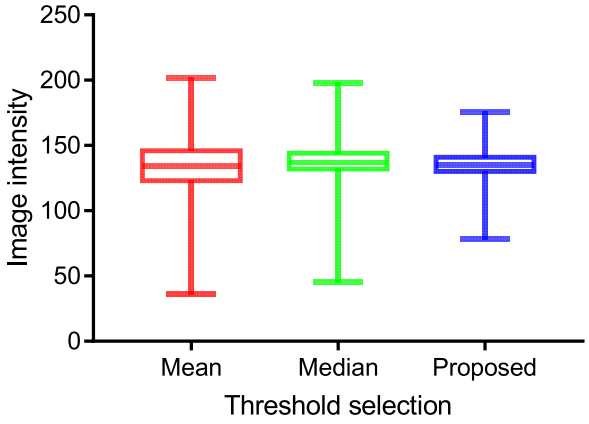

FIGURE 4. Comparison of mean and median based methods and proposed fuzzy-based method using box plots.

B. PERFORMANCE ANALYSIS

Before evaluating and comparing the subjective and objective performances of the proposed method with other contemporary HE methods, first consider the selection of threshold t for histogram partitioning. It is a established fact that the mean/median based histogram partitioned bi-HE methods do not give the the optimal performance in terms of all different metrics. In order to verify the fact that the best performing threshold for histogram partitioning is not necessarily mean or median intensity, Fig. 4 compares the box-plots of various thresholds selection methods for 1000 test images. Observing the size of the boxes, it can be stated that, the proposed fuzzy method produces different threshold values for 1000 test images compared to mean/median of the images, but the overall means of all three methods are close to each other which strengthen our hypothesis. Furthermore, the p-value of Kruskal-wallis one way ANOVA test [42] is used to analyse the statistical variance in means of three populations. Applying ANOVA test on the data obtained from 1000 test images, it is found that, the p-values for mean threshold vs. proposed threshold is 0.61 and for median threshold vs. proposed threshold is 0.66. In this case, the null hypothesis is that, the mean values of population for all three methods are equal. Since the obtained p-value is greater than the significance level of 1%, there is not enough evidence to reject the null hypothesis; and it can be concluded that, the proposed fuzzy method segments the histogram (and the image) with threshold not exactly at mean/median of image intensity, but it lies very close to the mean/median values.

TABLE 2. Average mean, SD, E, and EBCM of ID0001, ID0002, ID0003, ID0004, 100 training and 1000 test images.

Images	Mean	SD	E (bits)	EBCM
ID0001	115.58	30.45	6.83	0.15
ID0002	93.45	19.64	6.29	0.08
ID0003	94.38	39.06	6.89	0.06
ID0004	199.22	35.72	6.80	0.02
100 training images	131.27	35.81	6.62	0.20
1000 test images	136.26	45.56	6.55	0.13

TABLE 3. Comparison of various HE methods in terms of six different metrics.

Image	HE methods	AMBE	SD	E (bits)	PSNR (dB)	UIQ	EBCM
ID0001	CHE	11.89	**74.77**	5.94	16.39	0.76	0.28
	BBHE	**2.48**	73.20	**6.72**	17.95	0.78	**0.34**
	DSIHE	3.17	**73.84**	6.71	17.47	0.78	0.30
	BHEPL	4.10	58.98	6.70	17.90	0.76	**0.33**
	BHEPL-D	**1.95**	57.38	**6.72**	17.95	0.77	**0.32**
	BPDFHE	2.79	52.93	6.67	22.47	**0.86**	0.23
	SDDMHE-M	6.37	41.94	**6.83**	**33.93**	**0.93**	0.14
	SDDMHE-D	6.39	41.90	**6.83**	**34.02**	**0.93**	0.14
	TDCHE-M	2.79	43.27	6.69	**22.98**	0.81	0.21
	Proposed	**2.75**	**73.48**	6.71	17.88	0.78	0.31
ID0002	CHE	33.90	**74.62**	5.75	14.54	0.63	0.16
	BBHE	12.78	**74.13**	6.19	15.61	0.63	**0.17**
	DSIHE	16.15	**74.33**	6.19	15.54	0.63	**0.19**
	BHEPL	13.43	56.98	6.19	15.25	0.61	0.14
	BHEPL-D	11.98	56.58	**6.20**	16.07	0.65	**0.17**
	BPDFHE	**4.23**	59.44	6.10	18.87	0.72	0.14
	SDDMHE-M	**11.44**	34.34	**6.29**	**26.84**	**0.89**	0.07
	SDDMHE-D	**11.45**	34.37	**6.29**	**27.02**	**0.89**	0.08
	TDCHE-M	12.03	36.18	6.25	**20.73**	**0.74**	0.10
	Proposed	12.58	74.11	6.19	15.61	0.62	**0.19**
ID0003	CHE	33.08	**74.81**	5.96	14.29	0.73	**0.11**
	BBHE	**0.63**	71.85	6.87	**24.20**	**0.93**	**0.10**
	DSIHE	9.90	**73.05**	6.87	19.79	0.88	0.09
	BHEPL	**0.66**	57.64	6.85	19.60	0.86	0.08
	BHEPL-D	0.83	56.83	6.86	24.01	0.89	0.09
	BPDFHE	7.18	51.61	6.51	19.83	0.77	0.06
	SDDMHE-M	9.96	60.94	**6.89**	**29.03**	**0.92**	0.06
	SDDMHE-D	9.98	60.93	**6.89**	**29.10**	**0.92**	0.06
	TDCHE-M	6.85	51.57	6.86	22.78	0.91	0.06
	Proposed	**0.62**	**72.77**	**6.88**	23.73	**0.92**	**0.11**
ID0004	CHE	71.79	**74.76**	5.90	9.88	0.49	**0.10**
	BBHE	18.16	71.16	6.68	16.27	0.76	0.05
	DSIHE	30.36	**72.92**	6.62	17.96	0.74	**0.06**
	BHEPL	25.04	70.60	6.65	17.66	0.62	0.05
	BHEPL-D	12.70	51.70	6.68	18.19	0.82	0.04
	BPDFHE	19.55	65.49	4.65	13.44	0.46	**0.08**
	SDDMHE-M	**3.50**	38.03	**6.78**	**24.28**	**0.91**	0.02
	SDDMHE-D	**3.40**	38.09	**6.77**	**23.63**	**0.92**	0.02
	TDCHE-M	**7.60**	42.86	**6.72**	**20.04**	**0.83**	0.04
	Proposed	12.76	**73.20**	6.70	18.39	0.82	0.05

In order to compare the performance of proposed fuzzy bi-HE method with other contemporary methods such as CHE [7], BBHE [10], DSIHE [11], BHEPL [43], BHEPL-D [44], BPDFHE [23], SDDMHE-M [20], SDDMHE-D [20] and TDCHE-M [21], again the same data set of 1000 test images is used. Among the considered methods, BBHE and DSIHE are the simplest bi-HE methods and use mean and median intensity values of input image as

(a) Original (b) CHE (c) BBHE

(d) DSIHE (e) BHEPL (f) BHEPL-D

(g) BPDFHE (h) SDDMHE-M (i) SDDMHE-D

(j) TDCHE-M (k) Proposed

FIGURE 5. Results of various HE methods for ID0001 image.

threshold for histogram segmentation. On the other hands, BHEPL and BHEPL-D are the bi-HE methods that use pre-histogram controller to modify the segmented sub-histograms before the histogram equalisation. Similarly, among the multi-HE methods, BPDFHE is a simple threshold based fuzzy HE method, while SDDMHE's and TDCHE-M methods modify the segmented histograms before the equalisation. The detailed subjective analysis is presented for four images, whereas six metrics namely AMBE, SD, E, PSNR, UIQ and EBCM, are used for the objective analysis. The statistical

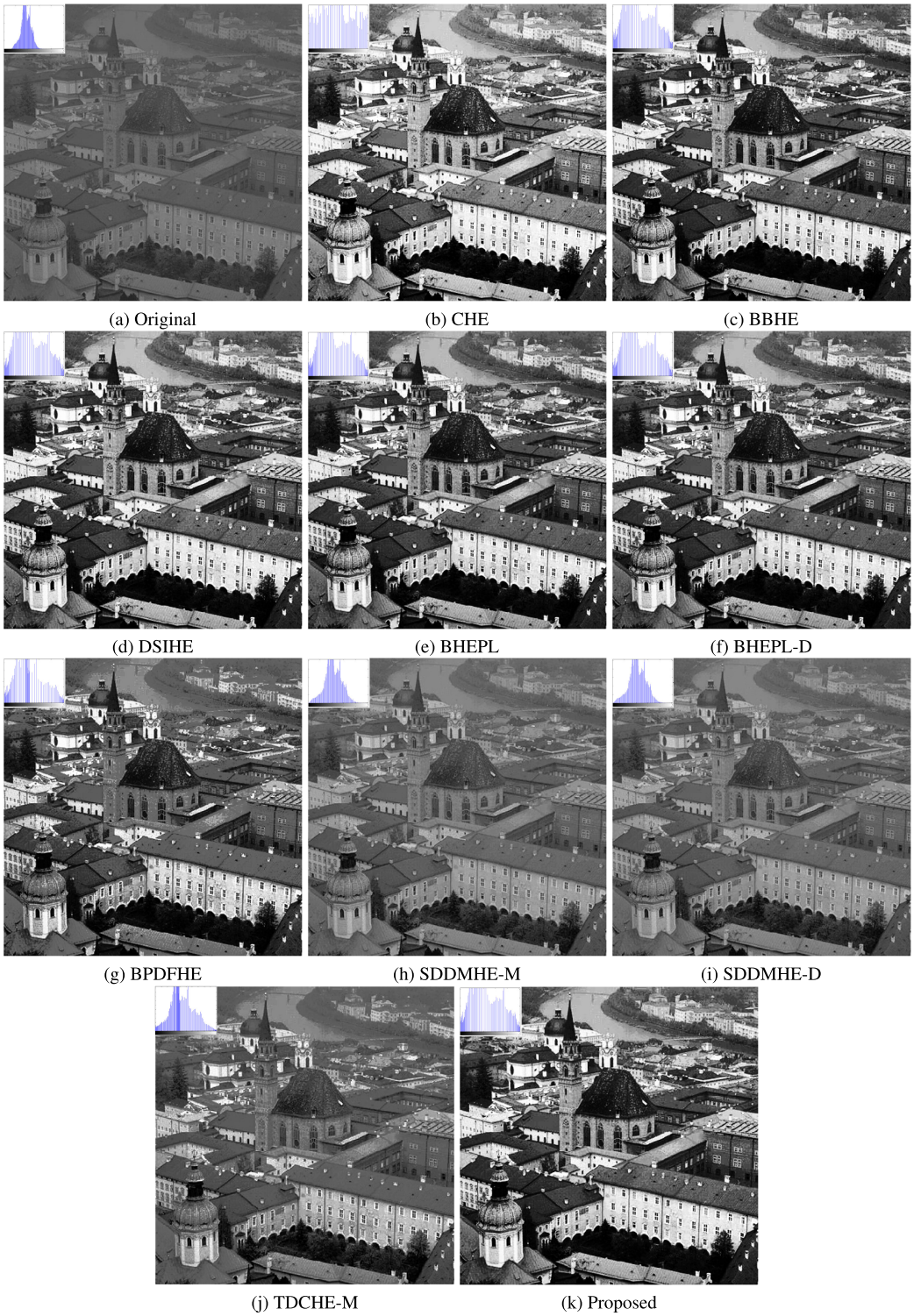

FIGURE 6. Results of various HE methods for ID0002 image.

and some objective parameters of 100 training images and 1000 test images along with that of four sample images (ID0001, ID0002, ID0003 and ID0004) are listed in Table 2.

The image ID0001 shown in Fig. 5(a) is a low contrast mid tone image consisting of lesser number of dark and bright pixels. Figs. 5(b)-(f) and (k) show images equalised using CHE and various bi-HE methods namely BBHE, DSIHE, BHEPL, BHEPL-D and the proposed method, whereas Figs. 5(g)-(j) show the images processed using fuzzy BPDFHE and multi-level non-fuzzy HE methods such as

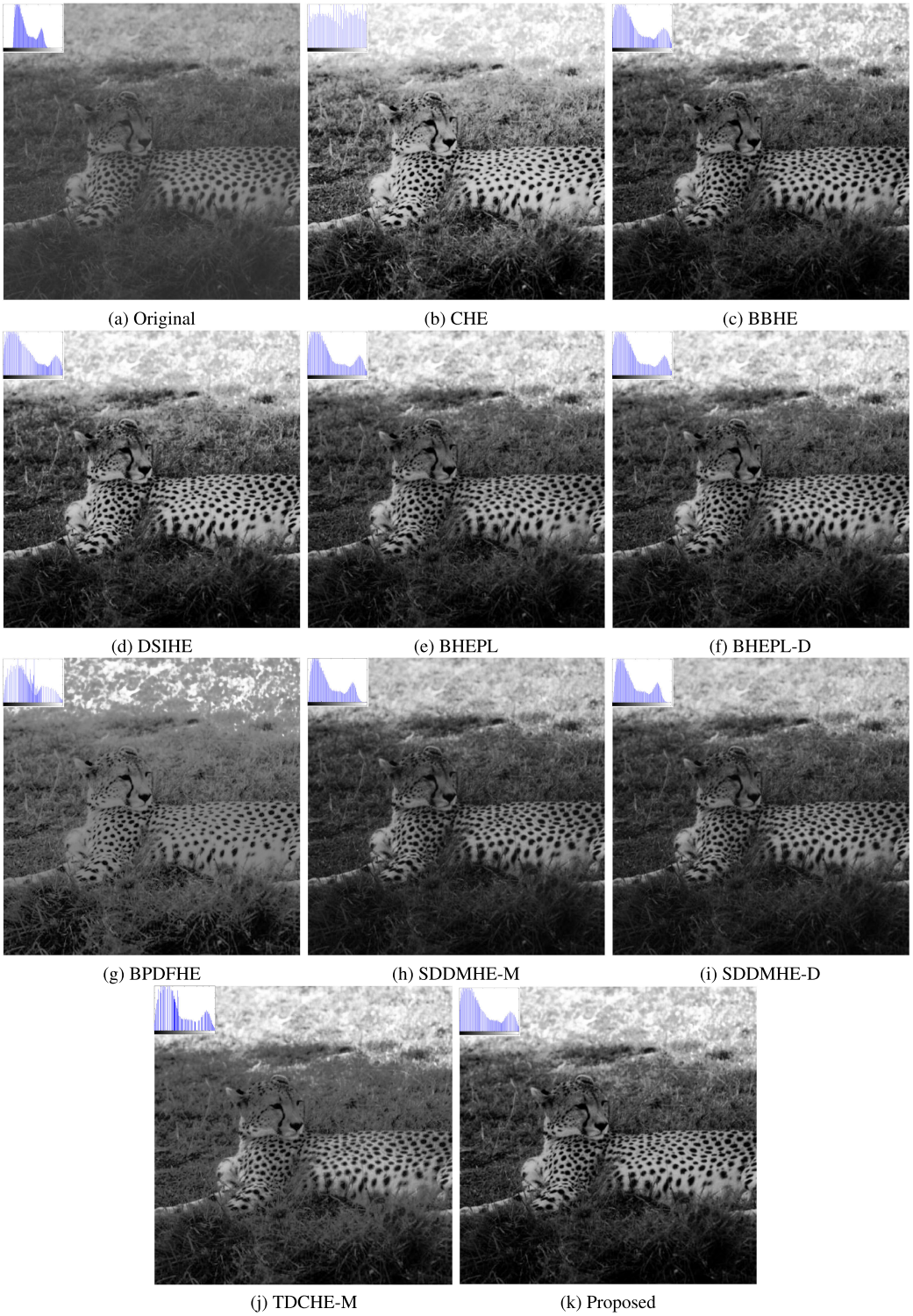

FIGURE 7. Results of various HE methods for ID0003 image.

SDDMHE-M, SDDMHE-D and TDCHE-M methods respectively. The corresponding normalised histograms for each method is shown at top left corner within each image. From Figs. 5(b)-(f) and (k), it can be observed that the histograms of bi-HE methods have better expansion of intensities. Among the multi-HE methods, BPDFHE has improper expansion of bins, thereby suffers with non-linear enhancement problem. This is due to the facts that this method selects peak-based thresholds lying closer to each other and therefore it fails to utilise the entire dynamic range for enhancement, which is

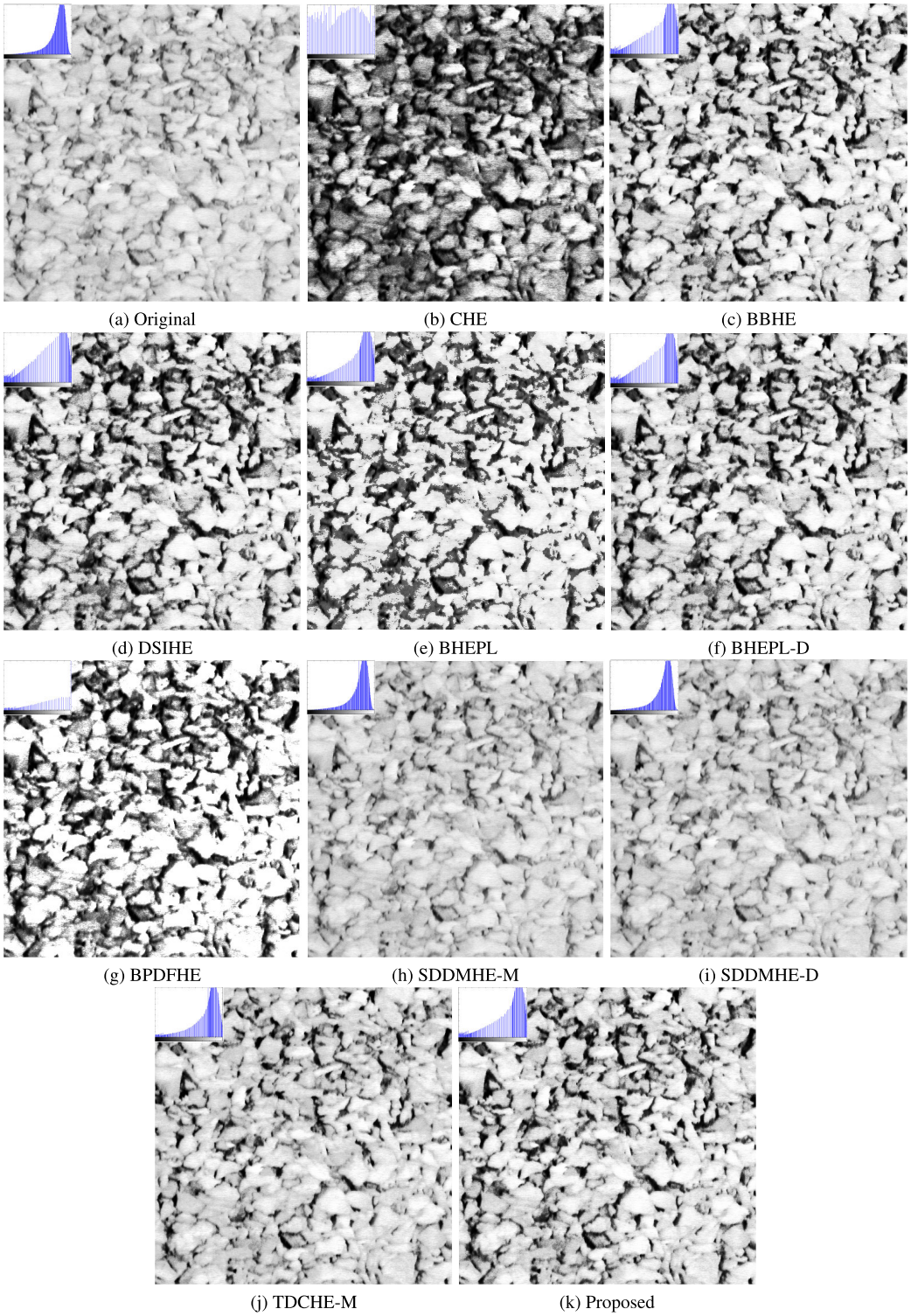

FIGURE 8. Results of various HE methods for ID0004 image.

evident from Figs. 5(g), as the higher intensity values have almost negligible presence. Although SDDMHE methods (for $n = 2$, $w = 10$) have better control on saturation artifacts and have uniform expansion of bins, as evident from corresponding histograms shown in Figs. 5(h) and (i). However, these methods do not offer any control mechanism to utilise full dynamic range for better contrast enhancement. Observing the image illustrated in Fig. 5(j) and respective histogram processed by TDCHE-M method, it can be perceived that this method failed to optimally select the thresholds

TABLE 4. Comparison of various HE methods in terms of average values (for 1000 test images) of AMBE, SD, E, PSNR, UIQ, EBCM and total execution time.

HE methods	Average AMBE	Average SD	Average E (bits)	Average PSNR (dB)	Average UIQ	Average EBCM	EBCM(O) ≥EBCM(I)	Total time (sec)
CHE	12.01	**75.26**	5.67	18.38	0.68	**0.21**	**981**	**309**
BBHE	10.79	**73.46**	6.44	19.29	0.72	**0.19**	969	**364**
DSIHE	9.50	**74.49**	6.44	19.45	0.71	**0.19**	**974**	**381**
BHEPL	15.99	62.15	6.43	17.19	0.78	0.18	**973**	532
BHEPL-D	10.10	58.67	**6.46**	19.96	0.75	0.18	970	573
BPDFHE	**8.24**	56.83	6.29	22.83	0.79	0.14	653	1984
SDDMHE-M	**5.73**	49.40	**6.53**	**34.02**	**0.90**	0.13	831	496
SDDMHE-D	**5.71**	50.39	**6.53**	**34.79**	**0.91**	0.13	708	512
TDCHE-M	13.19	52.71	5.84	**24.49**	0.77	0.16	926	794
Proposed	10.58	70.25	6.21	23.37	**0.83**	0.16	947	557

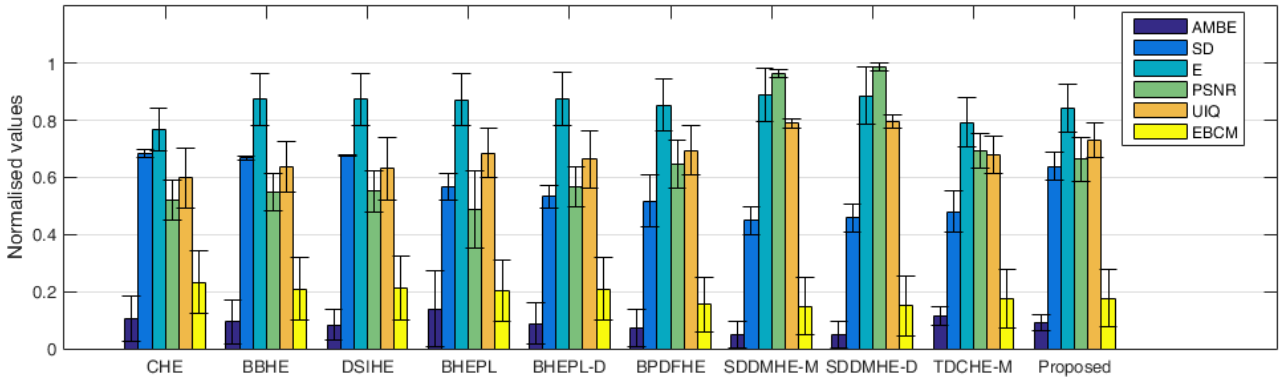

FIGURE 9. Normalised bar plots of various HE methods for different metrics.

for segmenting, which leads to the problem of non-linear enhancement of images. Similar observations can also be inferred from Figs. 6 and 7 for ID0002 and ID0003 images respectively.

The test image ID0004 illustrated in Fig. 8 is a brighter and textured image, as evident from the mean brightness value and peaks in the histogram. The main reason of considering such a textured image is that such images are relatively more prone to the over enhancement during the equalisation process, and it is worth investigating the performance of proposed method for such images. A close observation of Figs. 8(b)-(k) reveals that CHE, DSIHE, BHEPL and BPDFHE methods fail to efficiently enhance the contrast and the output image suffered from over enhancement problem, whereas the SDDMHE-M and SDDMHE-D methods are unable to enhance the image details as evident by comparing the histograms of input and processed images. On the other hand, BBHE, TDCHE-M and proposed methods have comparatively better enhancement control which can be observed from upper-left and lower-right regions of respective images.

As stated earlier the objective of proposed method is to select a threshold for histogram partitioning in bi-HE process that gives close to the best performance for all six metrics used in this work. In order to verify that the proposed method achieves this objective, Table 3 presents the quantitative comparison of the proposed method with other methods mentioned earlier in terms of six metrics namely AMBE, SD, E, PSNR, UIQ and EBCM for ID0001, ID0002, ID0003 and ID0004 images, whereas Table 4 shows average values (averaged for 1000 test images) of all six metrics along with total execution time, obtained using various HE methods. The best three results in Tables 3 and 4 are being shown in boldface. Observing Table 3, it can be asserted that the proposed method performs well for ID0003 image for five metrics, while the best performance of proposed algorithm limits to only one metric for ID0002 image but the value of other metrics like AMBE, SD and E are very close to third best parameter values. A very similar scenario as that of ID0002 is also observed for ID0001 and ID0004 images. It is worth noting that, the main reason behind good performance of image ID0003 is due to adjacency of a threshold value at which ID0003 gives best performance with the trade-off values of l^- and l^+. The proposed algorithm can be explicitly extended to different areas and its best performance can be elementarily achieved by precluding metrics that are outliers from best performing core metrics.

Note that, it is not equitable to limit the performance evaluation of any algorithm to only four images, hence it

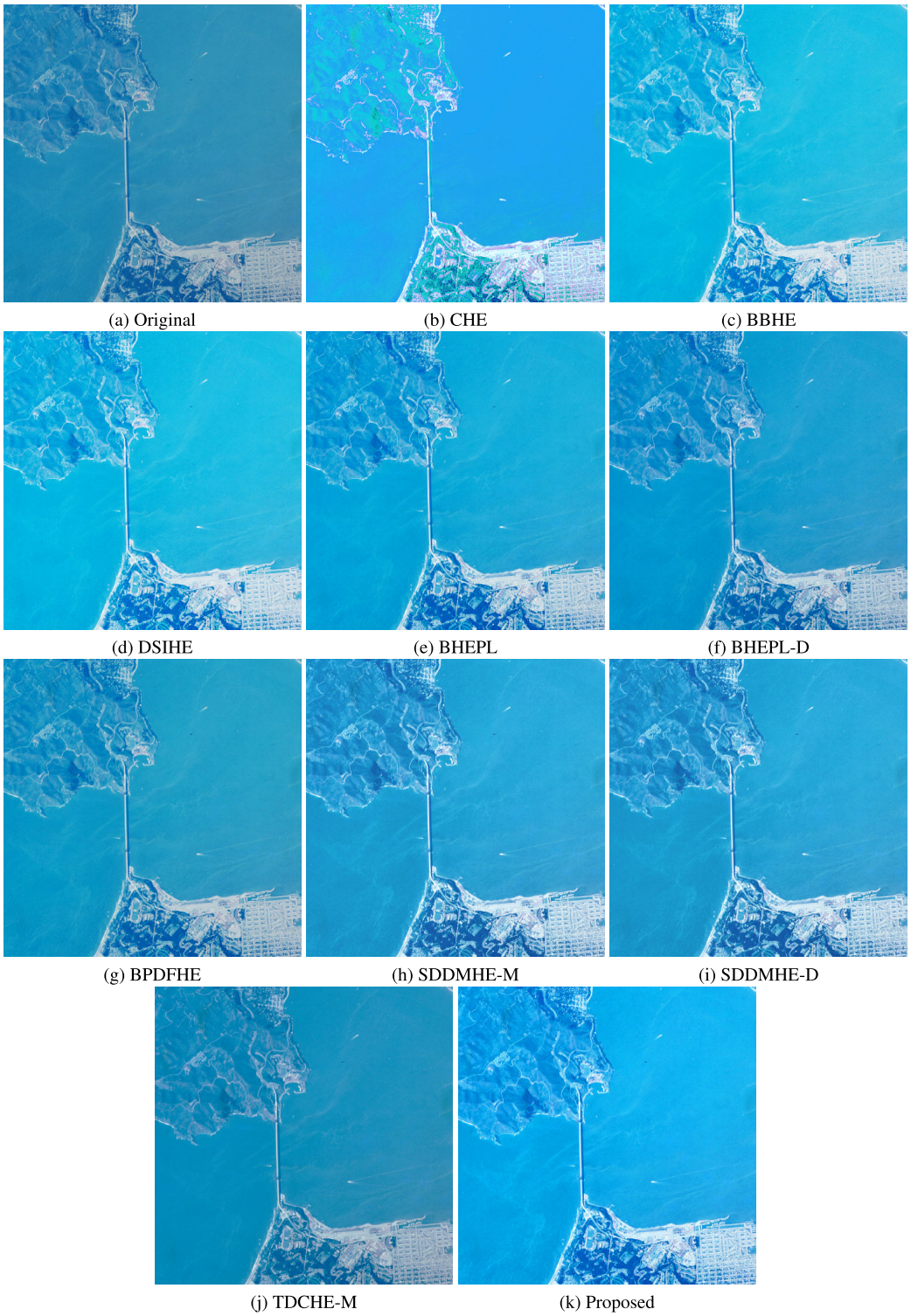

FIGURE 10. Results of various HE methods for San Francisco (Golden Gate) image.

is beneficial to expand the overall performance evaluation from four images to average of 1000 images. From Table 4, it can be observed that the proposed method gives the performance close to the best value for each parameter, whereas other methods achieve the best performance in terms of few parameters only and suffers with comparatively less satisfactory performance in terms of remaining parameters. For example, among all HE methods used for comparison purpose, SDDMHE methods have the best performance in terms of AMBE, E, PSNR and UIQ, as these methods

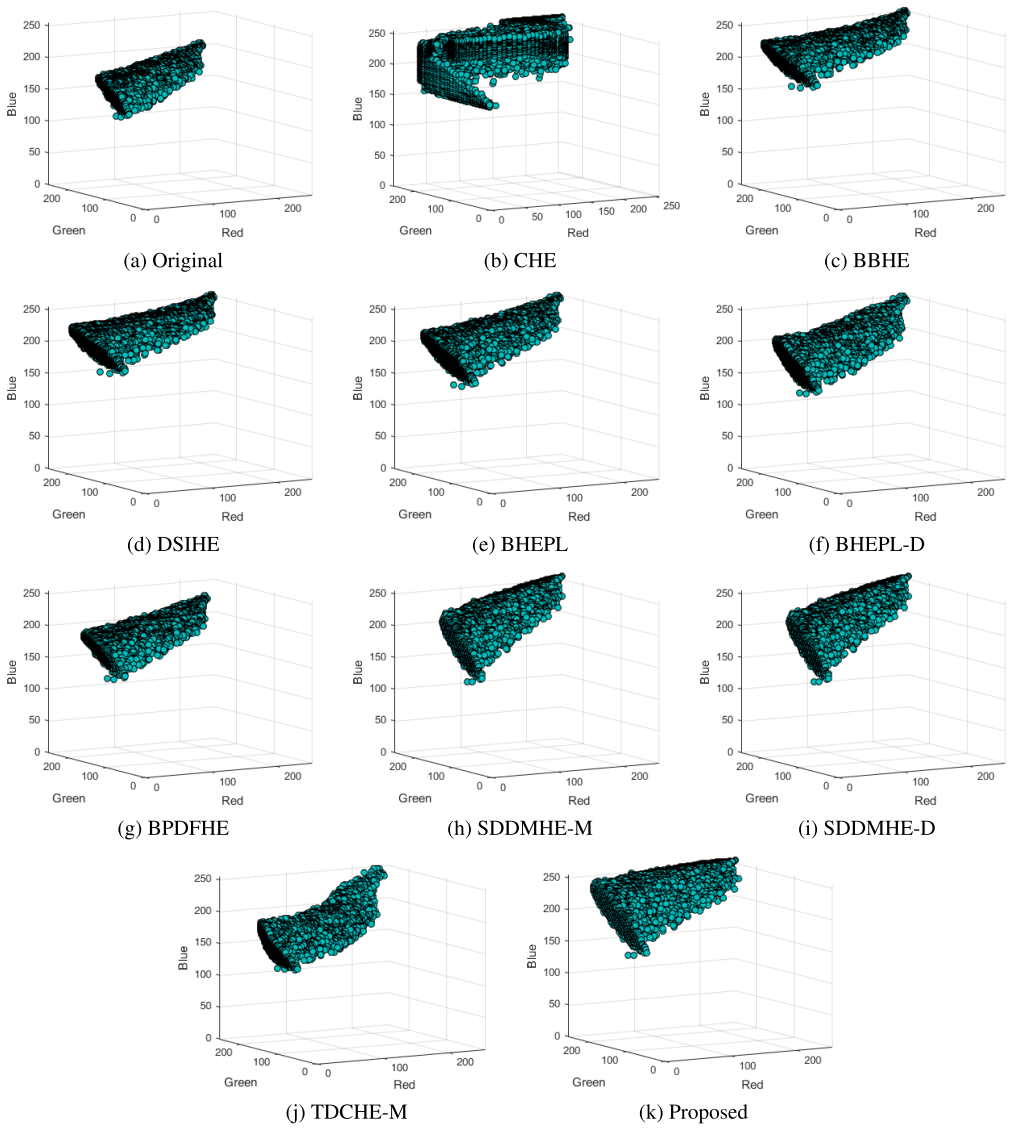

FIGURE 11. Image represented in the form of 3D RGB scatter plot for various HE methods for San Francisco (Golden Gate) image.

use normalisation function derived from the input image. However due to the normalisation of intensities SDDMHE methods fail to enhance the contrast effectively and hence have relatively lower values of SD and EBCM. Similarly, BBHE and DSIHE methods have superior performance in terms of SD and EBCM, but have relatively less satisfactory performance in terms of other parameters such as PSNR and UIQ. On the other hand, the proposed method gives near-best performance for all parameters.

Since proposed method is fuzzy-based, it is fair to compare its performance with other fuzzy-based HE methods. For this purpose, BPDFHE [23] method is used for performance comparison, which is a fuzzy based multi-HE method. Although BPDFHE method effectively preserves the mean brightness of the images compared to other HE methods, it is one of the most computationally expensive method due to the multiple segmentation process which is evident from Table 4. In contrast, as evident from Table 4, the proposed method outperforms the BPDFHE method in terms six metrics (out of eight) that excludes AMBE and E. Comparison of BBHE, DSIHE and proposed method in Table 4 reveals that the performances of these methods in terms of ABME, SD, E and EBCM are very close to each other, while performance difference is high for PSNR and UIQ. Note that, in order to compare the objective quality of images processed by various HE methods, two metrics namely PSNR and UIQ are used. Higher the value of these metrics, better is the image quality. The percentage score of the proposed method in terms of higher output EBCM value compared to its input is 94.7%.

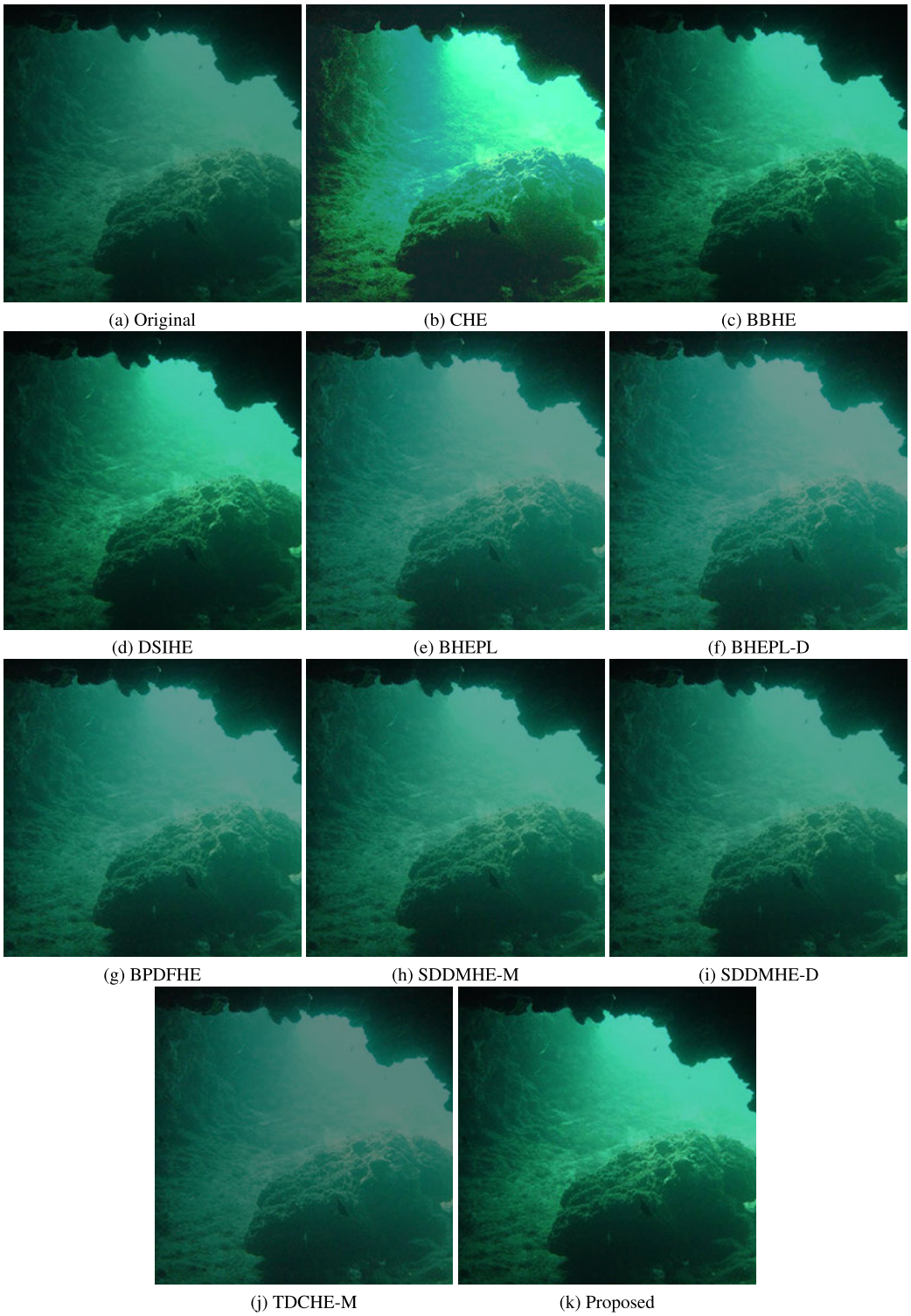

FIGURE 12. Results of various HE methods for underwater image.

Finally, to compare the computational complexity of various methods average execution time of each algorithm is also recorded in Table 4. It is observed that the proposed method has relatively higher complexity compared to CHE, BBHE and DSIHE, but it is comparable to other methods. The reason of higher complexity is due to searching of an optimal threshold by using two differently skewed level-snip MFs and finding the average value.

In order to further strengthen our claim that the proposed method gives the performance very close to the best value in

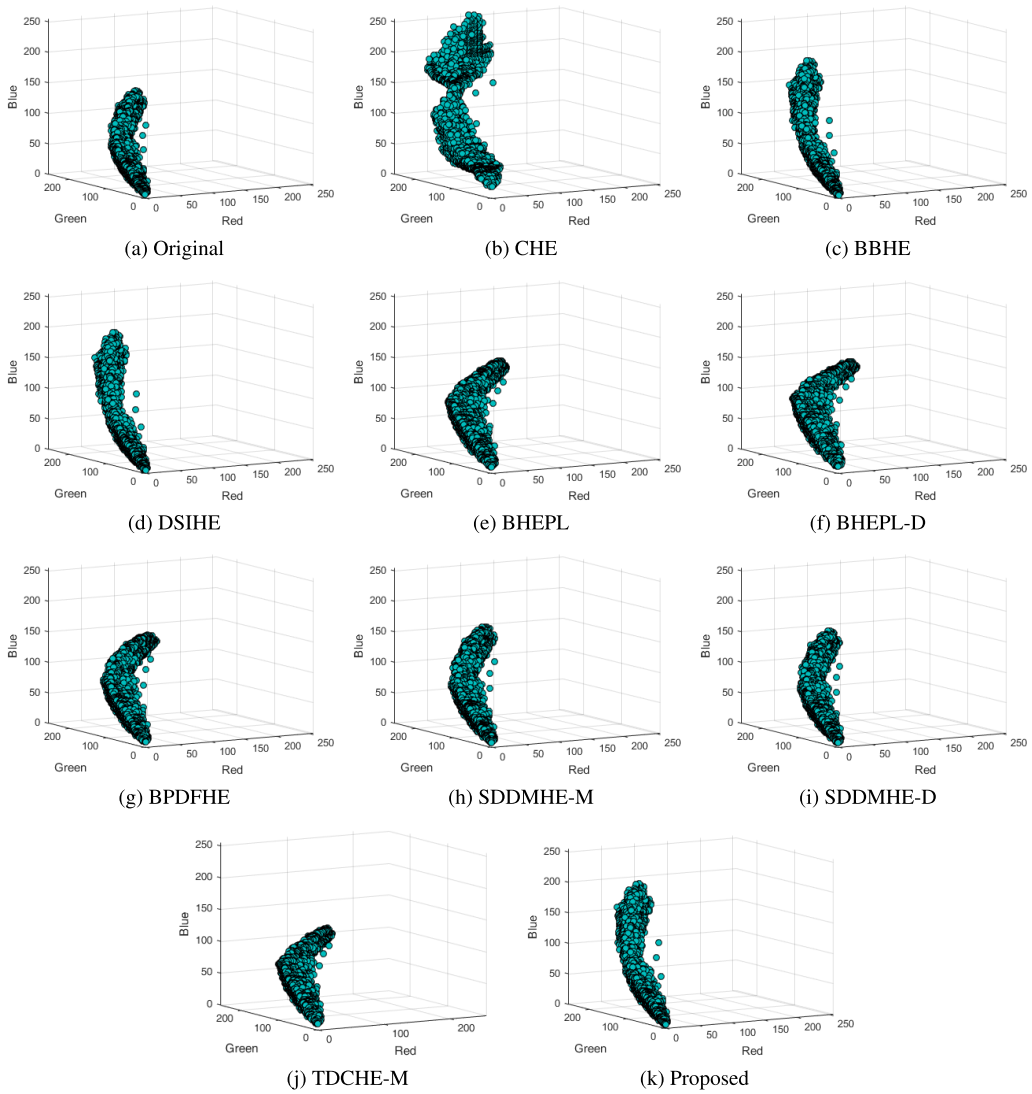

FIGURE 13. Image represented in the form of 3D RGB scatter plot for various HE methods for underwater image.

terms of majority of metrics, normalised bar plots comparing relative performance of all HE methods in terms of six metrics (namely AMBE, SD, E, PSNR, UIQ and EBCM) are shown in Fig. 9. Note that bar peak represents mean value and error bar represents standard deviation of the corresponding metric. A detailed analysis reveals that SDDMHE-D methods have the best performance in terms of AMBE, E, PSNR and UIQ, whereas CHE method gives the best performance in terms of SD and EBCM, and all other HE methods have their performance in between that of these two HE methods. Recall that, the objective of the proposed algorithm is to offer an optimal performance in terms of all metrics, which is very much justified from Fig. 9. For example, if we set a level of 0.6 in Fig. 9, then the advantage of proposed method can be highlighted. It can be observe that at this level the proposed method has mean values of four metrics namely SD, E, PSNR and UIQ above 0.6, while other HE methods have only either two or three metrics over it. Thus the bar plot analysis verifies and confirms that the proposed method though is not the best, but it gives the optimal performance which is very close to the best for all metrics.

IV. COLOR IMAGE ENHANCEMENT

The proposed method which is primarily being developed for gray scale images, can be easily extended to the colour images. For this purpose RGB image are first transformed to HSV colour space [45], [46]. Then the proposed method is applied on luminance component (V) only, and the unprocessed chrominance components are later combined. Finally, the inverse transformation is performed to obtain the enhanced RGB image. Fig. 10 shows the contrast enhancement of the San Francisco (Golden Gate) image using proposed method. From Fig. 10, it can be observed that the proposed fuzzy method with values of l^- and l^+ equal to

TABLE 5. Comparison of naturalness quality of processed images in terms of BRISQUE and NIQE.

HE methods	San Francisco image		Underwater image	
	BRISQUE	NIQE	BRISQUE	NIQE
CHE	22.3911	5.7024	2.6596	3.9114
BBHE	15.1999	4.7585	0.9849	**3.4161**
DSIHE	14.9844	4.8204	1.4944	**3.4857**
BHEPL	**13.9532**	4.8418	0.6687	3.7729
BHEPL-D	**14.4366**	**4.6373**	2.6596	3.7180
BPDFHE	16.0683	4.8175	5.4384	3.6615
SDDMHE-M	17.0276	4.7966	**0.4136**	3.5566
SDDMHE-D	17.1124	4.7961	**0.5789**	3.5949
TDCHE-M	18.4891	**4.2515**	7.4966	3.8149
Proposed	**12.7137**	**4.3172**	**0.4768**	**3.4383**

0.1385 and 0.2515 respectively, when applied on V component, enhances the image contrast without introducing saturation artifacts and the resultant image is qualitatively similar to that of images enhanced by BBHE and DSIHE methods.

Fig. 11 shows the 3D RGB scatter plot for various HE methods, which demonstrates the expansion of histogram to optimal level. From Fig. 11(a) it can be observed that points are clustered in a small area, which indicates the low contrast of the original image. As the image contrast is enhanced, the area of the accumulation increases. Note that, among all HE methods, only CHE has changed the characteristics for the original image to higher extent (refer Fig. 11(b)). Observing the plots of all equalised images i.e. Figs. 11(b)-(k), it can be stated that the proposed method has efficiently improved the contrast of the image and stretched the scatter plot efficiently over the dynamic range without distorting the characteristics of the original image.

Similar observations can also be made for a low contrast underwater image shown in Fig. 12. The underwater image is mostly composed of high percentage of green colour and it is difficult to achieve contrast enhancement for such images [47]. Observing the conventionally equalised image, it can be asserted that CHE method has saturated the intensities of the image and distorted its original characteristics which is also evident from corresponding scatter plot shown in Fig. 13(a). On the other hand, BBHE and DSIHE methods, including the proposed method have efficiently enhanced the image contrast, whereas BHEPL and BHEPL-D methods has limited contrast enhancement capability. Furthermore, a close observation of scatter plots illustrated in Figs. 13(c), (d) and (k) suggest that the proposed method on underwater image has resulted into slightly broader expansion of scatter plot compared to that of BBHE and DSIHE methods. So it can be stated that the proposed method has an ability to efficiently enhance the contrast of the image while preserving its original characteristics.

In order to evaluate the objective distortion in the natural appearance of the colour images during enhancement process, two metrics namely Blind/Referenceless Image Spatial Quality Evaluator (BRISQUE) [48] and Natural Image Quality Evaluator (NIQE) [49] are considered. Note that, both the metrics are based on the assumption that the natural images are comprised of some specific statistical properties, such as the luminance coefficients of natural images follow Gaussian-like distribution etc., which modifies during transformation process [48]. Hence, the least value of BRISQUE and NIQE represents comparatively less distortion in the statistical properties during enhancement process. Observing Table 5, it can be asserted that the proposed method is able to enhance the colour images without distorting the properties related to its natural appearance.

V. CONCLUSION

In this paper, it has been highlighted that the mean/median based histogram segmentation process do not always deliver the best performance in terms of all parameters used to quantify the performance of histogram equalisation. To overcome this problem, a novel fuzzy based bi-HE method is proposed, which ensures selection of a threshold for histogram partitioning using a level-snip technique, such that equalised image posses better visual characteristics. The simulation results suggest that the proposed method results in the quality of enhanced images comparable to that of mean/median based bi-HE methods. From the performance evaluation over wide range of images, it is observed that the proposed method delivers optimal contrast enhancement while preserving the information content and natural appearance of the image. This is due to the fact that the proposed method selects fuzzy threshold that offers optimal trade-off among various performance metrics. The proposed algorithm is inclusive and can be explicitly extended to different areas like remote sensing, underwater imaging, healthcare, security systems etc. The specific application of the proposed algorithm can be elementarily achieved by precluding metrics that are outliers from best performing core metrics. Further, the variables of the fuzzy MF such as l^-, l^+, a_1, a_2, and a_3 can be estimated using genetic algorithm or particle swarm optimization algorithm.

ACKNOWLEDGMENT

This work was supported by the Deanship of Scientific Research (DSR), King Abdulaziz University, Jeddah, under Grant DF-374-135-1441. The authors, therefore, gratefully acknowledge DSR technical and financial support.

REFERENCES

[1] C.-C. Ting, B.-F. Wu, M.-L. Chung, C.-C. Chiu, and Y.-C. Wu, "Visual contrast enhancement algorithm based on histogram equalization," *Sensors*, vol. 15, no. 7, pp. 16981–16999, Jul. 2015.

[2] C.-C. Chiu and C.-C. Ting, "Contrast enhancement algorithm based on gap adjustment for histogram equalization," *Sensors*, vol. 16, no. 6, p. 936, Jun. 2016.

[3] S. Fu, M. Zhang, C. Mu, and X. Shen, "Advancements of medical image enhancement in healthcare applications," *J. Healthcare Eng.*, vol. 2018, pp. 1–2, 2018.

[4] M. B. Nagarajan, M. B. Huber, T. Schlossbauer, G. Leinsinger, A. Krol, and A. Wismüller, "Classification of small lesions in dynamic breast MRI: Eliminating the need for precise lesion segmentation through spatio-temporal analysis of contrast enhancement," *Mach. Vis. Appl.*, vol. 24, no. 7, pp. 1371–1381, Oct. 2013.

[5] T. Saba, A. Rehman, Z. Mehmood, H. Kolivand, and M. Sharif, "Image enhancement and segmentation techniques for detection of knee joint diseases: A survey," *Current Med. Imag. Rev.*, vol. 14, no. 5, pp. 704–715, Sep. 2018.

[6] M. F. A. Hassan, A. S. A. Ghani, D. Ramachandram, A. Radman, and S. A. Suandi, "Enhancement of under-exposed image for object tracking algorithm through homomorphic filtering and mean histogram matching," *Adv. Sci. Lett.*, vol. 23, no. 11, pp. 11257–11261, Nov. 2017.

[7] R. C. Gonzalez and R. E. Woods, *Digital Image Processing*. Reading, MA, USA: Addison-Wesley, Apr. 1992.

[8] J. R. Tang and N. A. M. Isa, "Bi-histogram equalization using modified histogram bins," *Appl. Soft Comput.*, vol. 55, pp. 31–43, Jun. 2017.

[9] J.-Y. Kim, L.-S. Kim, and S.-H. Hwang, "An advanced contrast enhancement using partially overlapped sub-block histogram equalization," *IEEE Trans. Circuits Syst. Video Technol.*, vol. 11, no. 4, pp. 475–484, Apr. 2001.

[10] Y.-T. Kim, "Contrast enhancement using brightness preserving bi-histogram equalization," *IEEE Trans. Consum. Electron.*, vol. 43, no. 1, pp. 1–8, Feb. 1997.

[11] Y. Wang, Q. Chen, and B. Zhang, "Image enhancement based on equal area dualistic sub-image histogram equalization method," *IEEE Trans. Consum. Electron.*, vol. 45, no. 1, pp. 68–75, Feb. 1999.

[12] C. Wang and Z. Ye, "Brightness preserving histogram equalization with maximum entropy: A variational perspective," *IEEE Trans. Consum. Electron.*, vol. 51, no. 4, pp. 1326–1334, Nov. 2005.

[13] Z. Wei, H. Lidong, W. Jun, and S. Zebin, "Entropy maximisation histogram modification scheme for image enhancement," *IET Image Process.*, vol. 9, no. 3, pp. 226–235, Mar. 2015.

[14] X. Wang and L. Chen, "Contrast enhancement using feature-preserving bi-histogram equalization," *Signal, Image Video Process.*, vol. 12, no. 4, pp. 685–692, May 2018.

[15] L. Huang, W. Zhao, Z. Sun, and J. Wang, "An advanced gradient histogram and its application for contrast and gradient enhancement," *J. Vis. Commun. Image Represent.*, vol. 31, pp. 86–100, Aug. 2015.

[16] S. Li, W. Jin, L. Li, and Y. Li, "An improved contrast enhancement algorithm for infrared images based on adaptive double plateaus histogram equalization," *Infr. Phys. Technol.*, vol. 90, pp. 164–174, May 2018.

[17] S.-D. Chen and A. Ramli, "Contrast enhancement using recursive mean-separate histogram equalization for scalable brightness preservation," *IEEE Trans. Consum. Electron.*, vol. 49, no. 4, pp. 1301–1309, Nov. 2003.

[18] K. Sim, C. Tso, and Y. Tan, "Recursive sub-image histogram equalization applied to gray scale images," *Pattern Recognit. Lett.*, vol. 28, no. 10, pp. 1209–1221, Jul. 2007.

[19] M. F. Khan, E. Khan, and Z. Abbasi, "Segment selective dynamic histogram equalization for brightness preserving contrast enhancement of images," *Optik-Int. J. Light Electron Opt.*, vol. 125, no. 3, pp. 1385–1389, Feb. 2014.

[20] M. F. Khan, E. Khan, and Z. Abbasi, "Segment dependent dynamic multi-histogram equalization for image contrast enhancement," *Digit. Signal Process.*, vol. 25, pp. 198–223, Feb. 2014.

[21] M. Zarie, H. Hajghassem, and A. Eslami Majd, "Contrast enhancement using triple dynamic clipped histogram equalization based on mean or median," *Optik-Int. J. Light Electron Opt.*, vol. 175, pp. 126–137, Dec. 2018.

[22] M. F. Khan, E. Khan, and Z. Abbasi, "Image contrast enhancement using normalized histogram equalization," *Optik-Int. J. Light Electron Opt.*, vol. 126, no. 24, pp. 4868–4875, Dec. 2015.

[23] D. Sheet, H. Garud, A. Suveer, M. Mahadevappa, and J. Chatterjee, "Brightness preserving dynamic fuzzy histogram equalization," *IEEE Trans. Consum. Electron.*, vol. 56, no. 4, pp. 2475–2480, Nov. 2010.

[24] M. F. Khan, E. Khan, and Z. A. Abbasi, "Artifact suppressed image enhancement through bi histogram equalization," in *Proc. IEEE IMPACT*, Nov. 2013, pp. 66–70.

[25] V. Magudeeswaran and C. G. Ravichandran, "Fuzzy logic-based histogram equalization for image contrast enhancement," *Math. Problems Eng.*, vol. 2013, Jun. 2013, Art. no. 891864.

[26] M. F. Khan, X. Ren, and E. Khan, "Semi dynamic fuzzy histogram equalization," *Optik-Int. J. Light Electron Opt.*, vol. 126, no. 21, pp. 2848–2853, Nov. 2015.

[27] M. Farhan Khan, E. Khan, and Z. A. Abbasi, "Multi segment histogram equalization for brightness preserving contrast enhancement," in *Proc. Adv. Comput. Sci., Eng. Appl.*, 2012, pp. 193–202.

[28] M. F. Khan, E. Khan, and Z. A. Abbasi, "Weighted average multi segment histogram equalization for brightness preserving contrast enhancement," in *Proc. IEEE Int. Conf. Signal Process., Comput. Control*, Mar. 2012, pp. 1–6.

[29] M. F. Khan and M. A. Khan, "Information preserving histogram segmentation of low contrast images using fuzzy measures," *Optik-Int. J. Light Electron Opt.*, vol. 157, pp. 1397–1404, Mar. 2018.

[30] S. Lee, "An efficient content-based image enhancement in the compressed domain using retinex theory," *IEEE Trans. Circuits Syst. Video Technol.*, vol. 17, no. 2, pp. 199–213, Feb. 2007.

[31] S.-W. Jung, "Enhancement of image and depth map using adaptive joint trilateral filter," *IEEE Trans. Circuits Syst. Video Technol.*, vol. 23, no. 2, pp. 258–269, Feb. 2013.

[32] G. Raju and M. S. Nair, "A fast and efficient color image enhancement method based on fuzzy-logic and histogram," *AEU-Int. J. Electron. Commun.*, vol. 68, no. 3, pp. 237–243, Mar. 2014.

[33] M. Hanmandlu and D. Jha, "An optimal fuzzy system for color image enhancement," *IEEE Trans. Image Process.*, vol. 15, no. 10, pp. 2956–2966, Oct. 2006.

[34] M. S. Nair, R. Lakshmanan, M. Wilscy, and R. Tatavarti, "Fuzzy logic-based automatic contrast enhancement of satellite images of ocean," *Signal, Image Video Process.*, vol. 5, no. 1, pp. 69–80, Mar. 2011.

[35] K. Hasikin and N. A. M. Isa, "Adaptive fuzzy contrast factor enhancement technique for low contrast and nonuniform illumination images," *Signal, Image Video Process.*, vol. 8, no. 8, pp. 1591–1603, Nov. 2014.

[36] S. Zhou, F. Zhang, and M. A. Siddique, "Range limited peak-separate fuzzy histogram equalization for image contrast enhancement," *Multimed Tools Appl.*, vol. 74, no. 17, pp. 6827–6847, Sep. 2015.

[37] B. Subramani and M. Veluchamy, "Fuzzy contextual inference system for medical image enhancement," *Measurement*, vol. 148, Dec. 2019, Art. no. 106967.

[38] S. Jenifer, S. Parasuraman, and A. Kadirvelu, "Contrast enhancement and brightness preserving of digital mammograms using fuzzy clipped contrast-limited adaptive histogram equalization algorithm," *Appl. Soft Comput.*, vol. 42, pp. 167–177, May 2016.

[39] A. S. Parihar, O. P. Verma, and C. Khanna, "Fuzzy-contextual contrast enhancement," *IEEE Trans. Image Process.*, vol. 26, no. 4, pp. 1810–1819, Apr. 2017.

[40] T. Celik and T. Tjahjadi, "Automatic image equalization and contrast enhancement using Gaussian mixture modeling," *IEEE Trans. Image Process.*, vol. 21, no. 1, pp. 145–156, Jan. 2012.

[41] Z. Wang and A. Bovik, "A universal image quality index," *IEEE Signal Process. Lett.*, vol. 9, no. 3, pp. 81–84, Mar. 2002.

[42] D. J. Sheskin, *Handbook of Parametric and Nonparametric Statistical Procedures*. New York, NY, USA: CRC Press, 2007.

[43] C. Ooi, N. Pik Kong, and H. Ibrahim, "Bi-histogram equalization with a plateau limit for digital image enhancement," *IEEE Trans. Consum. Electron.*, vol. 55, no. 4, pp. 2072–2080, Nov. 2009.

[44] C. Ooi and N. A. M. Isa, "Adaptive contrast enhancement methods with brightness preserving," *IEEE Trans. Consum. Electron.*, vol. 56, no. 4, pp. 2543–2551, Nov. 2010.

[45] W. K. Pratt, *Digital Image Processing*. Hoboken, NJ, USA: Wiley, 2007.

[46] J. Ma, X. Fan, S. X. Yang, X. Zhang, and X. Zhu, "Contrast limited adaptive histogram equalization-based fusion in YIQ and HSI color spaces for underwater image enhancement," *Int. J. Pattern Recognit. Artif. Intell.*, vol. 32, no. 7, Jul. 2018, Art. no. 1854018.

[47] A. S. Abdul Ghani and N. A. M. Isa, "Enhancement of low quality underwater image through integrated global and local contrast correction," *Appl. Soft Comput.*, vol. 37, pp. 332–344, Dec. 2015.
[48] A. Mittal, A. K. Moorthy, and A. C. Bovik, "No-reference image quality assessment in the spatial domain," *IEEE Trans. Image Process.*, vol. 21, no. 12, pp. 4695–4708, Dec. 2012.
[49] A. Mittal, R. Soundararajan, and A. C. Bovik, "Making a completely blind image quality analyzer," *IEEE Signal Process. Lett.*, vol. 20, no. 3, pp. 209–212, Mar. 2013.

MOHAMMAD FARHAN KHAN received the B.Tech. and M.Tech. degrees in electronics engineering from the Z. H. College of Engineering and Technology, Aligarh Muslim University, India, in 2010 and 2012, respectively, and the Ph.D. degree in electronic engineering from the School of Engineering and Digital Arts, University of Kent, U.K., in 2017. He has worked as Postdoctoral Research Associate in the EPSRC funded project that was in joint collaboration between the University of Warwick, U.K., and the University of Central Lancashire, U.K. His research experiences include applied control theory, 2D/3D monitoring, image processing, mathematical modeling, soft computing, machine learning, artificial intelligence, and computational biology.

DEEPALI GOYAL received the M.Tech. degree in electronics engineering from Aligarh Muslim University, Aligarh, India, in 2015. Her research experiences include image processing and soft computing.

MUAFFAQ M. NOFAL received the B.S. and M.S. degrees in physics from the University of Jordan, in 1991 and 1995, respectively, and the Ph.D. degree in experimental atomic physics from Frankfurt University, Germany, in 2007. From 2007 to 2009, he worked as an Assistant Professor with Applied Science University, Amman, Jordan. Since 2009, he has been an Assistant Professor with the Science Department, Prince Sultan University, Saudi Arabia.

EKRAM KHAN received the B.Sc.(Eng.) and M.Sc.(Eng.) degrees in electronics engineering from Aligarh Muslim University (AMU), Aligarh, India, in 1991 and 1994, respectively, and the Ph.D. degree in electronics engineering from the University of Essex, Colchester, U.K., in 2003. In 1993, he joined the Department of Electronics Engineering, AMU, where he has been a Professor, since 2009. He has successfully completed several research projects funded by various agencies in India and U.K. He spent the summer of 2005 and 2006, as an Academic Visitor, at the University of Essex (funded by the Royal Society, U.K). He has authored or coauthored more than 90 articles in refereed academic journals and international conference proceedings. His research interests include low-complexity image/video coding, video transmission over wireless networks, and biomedical image processing. He is also a Life Member of the Institution of Electronics and Telecommunication Engineers, India, and the Systems Society of India. He received the Commonwealth Scholarship to pursue the Ph.D. degree with the University of Essex. He also received the Research Award from the IBM J. T. Watson Research Laboratory, USA, for the best disruptive idea presented at the IEEE ICME 2002, held at EPFL, Switzerland.

RAMI AL-HMOUZ received the B.Sc. degree in electrical engineering from Mutah University, Alkarak, Jordon, in 1998, the M.Sc. degree in computer engineering from the University of Western Sydney, Sydney, NSW, Australia, in 2004, and the Ph.D. degree in computer engineering from the University of Technology, Sydney, NSW, in 2008. He is currently a Professor with King Abdulaziz University (KAU), Jeddah, Saudi Arabia. His research interests include machine learning, computer vision, and granular computing.

ENRIQUE HERRERA-VIEDMA received the M.Sc. and Ph.D. degrees in computer science from the University of Granada, Granada, Spain, in 1993 and 1996, respectively. He is currently a Professor of computer science with Data Science and Computational Intelligence, and the Vice-President for research and knowledge transfer with the University of Granada. His H-index is 69 with more than 18000 citations received in Web of Science and 85 in Google Scholar with more than 29000 cites received. He has been identified as one of the world's most influential researchers by the Shanghai Center and Thomson Reuters/Clarivate Analytics in both computer science and engineering in the years 2014–2018. His current research interests include group decision making, consensus models, linguistic modeling, aggregation of information, information retrieval, bibliometric, digital libraries, web quality evaluation, recommender systems, and social media. He is the Vice-President for Publications in SMC Society and an Associate Editor in several journals, such as the IEEE TRANSACTIONS ON FUZZY SYSTEMS, the IEEE TRANSACTIONS ON SYSTEMS, MAN, AND CYBERNETICS: SYSTEMS, *Information Sciences*, *Applied Soft Computing*, *Soft Computing*, *Fuzzy Optimization and Decision Making*, *International Journal of Fuzzy Systems*, the *Journal of Intelligent & Fuzzy Systems*, *Engineering Applications of Artificial Intelligence*, the *Journal of Ambient Intelligence and Humanized Computing*, the *International Journal of Machine Learning and Cybernetics*, and *Knowledge-Based Systems*.